Progress on Developing the Spherical Tokamak for Fusion Applications*

J. Menard[1], T. Brown[1], J. Canik[2], L. El-Guebaly[3], S. Gerhardt[1], S. Kaye[1], M. Kotschenreuther[4], R. Maingi[2], G.H. Neilson[1], C.L. Neumeyer[1], M. Ono[1], R. Raman[5], S. Sabbagh[6], V. Soukhanovskii[7], P. Titus[1], G. Voss[8], R. Woolley[1], A. Zolfaghari[1] and the NSTX Upgrade team[1]

[1]Princeton Plasma Physics Laboratory, Princeton, NJ, USA
[2]Oak Ridge National Laboratory, Oak Ridge, TN, USA
[3]University of Wisconsin, Madison, WI, USA
[4]University of Texas at Austin, Austin, TX, USA
[5]University of Washington, Seattle, WA, USA
[6]Columbia University, New York, NY, USA
[7]Lawrence Livermore National Laboratory, Livermore, CA, USA
[8]Culham Centre for Fusion Energy, Abingdon, Oxfordshire, United Kingdom

Corresponding Author: jmenard@pppl.gov

Abstract:

A Fusion Nuclear Science Facility (FNSF) could play an important role in the development of fusion energy by providing the high neutron flux and fluence environment needed to develop fusion materials and components. The spherical tokamak (ST) is a leading candidate for an FNSF due to its compact size and modular configuration. Two activities preparing the ST for possible FNSF applications have been advanced in the U.S. during the past two years. First, a major upgrade of the National Spherical Torus eXperiment (NSTX) has been designed, approved, and initiated, and physics and engineering design studies have been published [1, 2]. Second, previous "pilot plant" studies [3] identified key research needs and design issues for ST-based FNSF devices and have motivated studies of the impact of device size on neutron wall loading, tritium breeding, and electricity production. For example, for an ST-FNSF with average neutron wall loading of 1 MW/m^2, the impact of increased major radius is stabilizing, but the overall fusion power and tritium consumption increases. For higher performance operation targeting net electricity production, the smallest possible ST that can achieve electricity breakeven has R = 1.6 m assuming very high blanket thermal conversion efficiency. For these high power density devices, the divertor region is also a critical and challenging area, and a unique configuration has been identified in which divertor Cu PF coils are placed in the ends of the ST center-stack to enable high-triangularity plasma shapes with flux expansion of 15-20 compatible with demountable TF legs and a removable center-stack. Higher flux-expansions of 40-70 enabled by snowflake divertors have also been incorporated as means of further mitigating high heat flux and promoting detachment. An important issue is the impact of device size and blanket configuration on tritium breeding ratio (TBR) where smaller devices have more difficulty achieving TBR=1 since a higher fraction of in-vessel surface area must be dedicated to auxiliary heating ports and blanket test modules. Lastly, several blanket maintenance strategies are explored including removal in a single vertical lift and a segmented approach in which dedicated vertical ports are used to remove individual blanket segments.

*The author of this manuscript is supported by U.S. Dept. of Energy contract DE-AC02-09CH11466

1 Introduction

Previous studies identified a pilot plant as a potentially attractive next-step towards fusion commercialization by demonstrating generation of a small amount of net electricity as quickly as possible and in as small a facility as possible in a configuration directly scalable to a power plant [3]. The pilot plant approach could accelerate the commercialization of magnetic fusion by targeting electricity break-even while also carrying forward a high neutron fluence fusion nuclear science and technology (FNST) and component testing mission needed to ultimately achieve high availability in fusion systems. The pilot plant studies also identified a range of research needs which must be addressed before a pilot plant of any configuration (AT, ST, CS) could be pursued with a reasonable probability of fulfilling its mission. Further, for present ST pilot designs with normally conducting TF coils, resistive losses in the TF must be offset by increased device size and fusion power to achieve electrical break-even, and the resultant ST device sizes are comparable in size to the other configurations. However, as previously argued, if the electrical self-sufficiency constraint is softened or eliminated, the ST is a leading candidate for an FNSF due to its compact size and modular configuration [4, 5, 6, 7, 8].

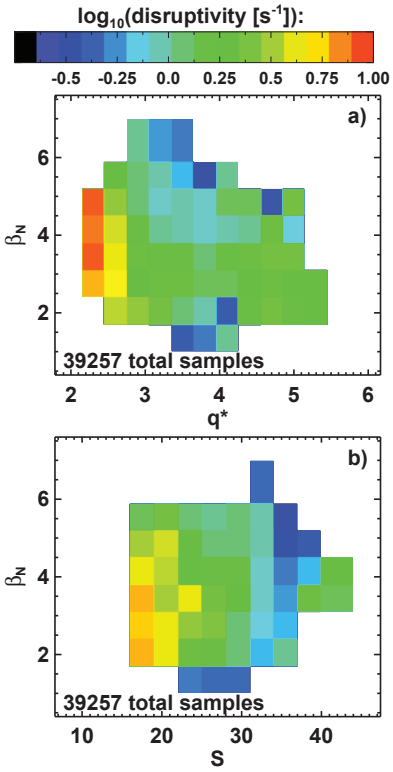

FIG. 1: NSTX disruptivity versus β_N and (a) kink safety factor q^* and (b) shaping factor S.

These considerations have motivated recent U.S. ST development studies to focus on a systematic exploration of the possible achievable missions as a function of device size. The study is considering sizes ranging from a small component test facility (CTF) (R≈1m) without a requirement for tritium self-sufficiency to a larger (R=2.2m) pilot plant capable of component testing, tritium self-sufficiency, and net electricity production. This study is presently focusing on a relatively unstudied size R=1.6m intermediate between previous FNSFs and a pilot plant. An important goal of the above review of configurations is to put the physics and engineering assumptions on a uniform footing, and to identify strengths and weaknesses of the various configurations in order to optimize ST-FNSF design.

The complete comparative study of different ST configurations is not yet complete and will be reported on at a future date. However, an important initial finding of the study is that some proposed ST devices may not have sufficient margin with respect to global plasma stability limits. In particular, as shown in Figure 1, disruptivity rates for NSTX plasmas are found to increase substantially for kink safety factor values $q^* < 2.6$ and for shaping factor $S \equiv q_{95} I_P / a B_T < 22$ [9]. Interestingly, there does not appear to be a trend of increased disruptivity for the highest NSTX β_N values of $4.5 - 6.5$, i.e. above the n=1 no-wall limit. This is likely due to the beam-driven toroidal rotation, wall stabilization, and active error field and RWM feedback control of NSTX [10]. Thus, based on present NSTX data, reduced disruptivity likely requires $q^* \geq 2.6$ and $S \geq 22$ in ST-FNSF designs.

2 FNSF Performance Dependence on Device Size

A fundamental constraint for FNSF devices is achievable neutron wall loading [11], and for the size variations studied here an average neutron wall loading of W_n = 1MW/m^2 is chosen. Based on previous design studies, the lower-bound on device size while remaining able to provide a sufficient component testing area of 10m^2 [11] is $R \approx$ 1m. The ST pilot plant study bounds the larger major radius considered here at R=2.2m. Device performance is computed at fixed neutron wall loading as a function of major radius assuming fixed aspect ratio A=1.7, elongation κ=3, B_T=3T, NNBI injection energy E = 500keV for heating and current drive, the ITER H-mode confinement multiplier H_{98} =1.2, and Greenwald density fraction $f_{Greenwald}$ =0.8. It should be noted that NNBI at E=500keV may be too energetic to be fully absorbed in smaller FNSF devices, and if lower energy is used, more power may be required (due to reduced current drive efficiency) to achieve the assumed NBI current drive.

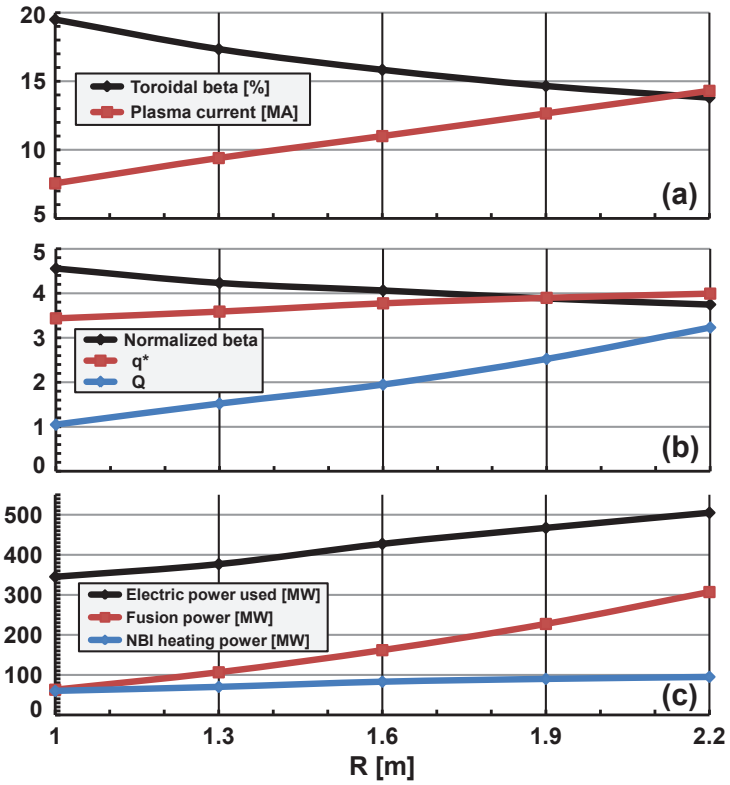

FIG. 2: ST-FNSF parameters versus device major radius at fixed average neutron wall loading = 1MW/m^2.

Figure 2 shows that as the plasma major radius R is increased from 1m to 2.2m, the impact is stabilizing, since β_T = 19.5% $\rightarrow$ 14%, β_N = 4.6 $\rightarrow$ 3.8, and q* = 3.4 $\rightarrow$ 4.0. However, the plasma current doubles from 7.5MA to 14.3MA and the fusion gain Q increases from 1 to 3. The fusion power increases from 60MW to 300MW and the tritium consumption also therefore increases by a factor of 5. The auxiliary heating power increases from 60 to 95MW, and the total electric power consumed increases from 350MW to 500MW assuming the same (and higher than presently achievable) wall-plug efficiency of 0.4 for NNBI as used in the pilot-plant study [3]. Higher energy confinement would reduce the auxiliary power required, increase Q, and reduce overall power consumption.

In the limit where tritium self-sufficiency is not required, clearly small STs are favored since they minimize fusion power and tritium consumption. However, tritium self-sufficiency and electrical self-sufficiency are ultimately required for the development of fusion energy, so it is important to determine the thresholds in device size for achieving these goals. Initial assessments of tritium self-sufficiency are described in Section 4. For electrical self-sufficiency, the engineering efficiency Q_{eng} (utilizing the same parametric as-

sumptions as in previous pilot plant studies [3]) is defined as the ratio of electrical power produced to electrical power consumed and can be expressed as:

$$Q_{eng} = \frac{\eta_{th}\eta_{aux}Q(4M_n + 1 + 5/Q + 5P_{pump}/P_{fus})}{5(1 + \eta_{aux}Q(P_{pump} + P_{sub} + P_{coils} + P_{control})/P_{fus})} \quad (1)$$

where η_{th} = thermal conversion efficiency, η_{aux} = auxiliary power wall plug efficiency, P_{fus} = total DT fusion power, P_{aux} = auxiliary power for heating and current-drive, $Q = P_{fus}/P_{aux}$, M_n = neutron energy multiplier, P_{th} = thermal power = $M_nP_n + P_\alpha + P_{aux}$, P_{pump} = coolant pumping power, P_{sub} = subsystems power, P_{coils} = power lost in normally conducting coils, and $P_{control}$ = power used in plasma or plant control not included in P_{aux}. Equation 1 illustrates that the leading terms in the engineering efficiency Q_{eng} involve a combination of technology and physics performance metrics. In particular, Q_{eng} depends to leading order on the thermal conversion and auxiliary system wall-plug efficiencies (η_{th} and η_{aux}) and the fusion gain Q. To achieve electrical self-sufficiency in the modest-sized ST devices considered here requires high blanket thermal conversion efficiency, decreased toroidal field, and increased confinement and stability. For this analysis, the value of η_{th} is varied to assess the impact on Q_{eng}, a constant $\eta_{aux} = 0.4$ is assumed, the normalized current drive (CD) efficiency $\eta_{CD} = I_{CD}R_0n_e/P_{CD} = 0.3 \times 10^{20}A/Wm^2$, and $M_n = 1.1$.

Figure 3 shows the engineering efficiency and fusion gain Q for a range of blanket thermal conversion efficiencies and device sizes for high-performance ST-FNSF scenarios targeting net electricity production. These scenarios have fixed B_T = 2.6T, H_{98}=1.5, β_N = 6, β_T = 35%, and q^* = 2.5. Such scenarios have normalized confinement and stability performance near or at the highest values achieved on NSTX. In the size scan in Figure 3, the Greenwald fraction is allowed to vary to keep the above parameters constant, and f_{GW} decreases from approximately 0.66 for R=1-1.6m to 0.56 and 0.47 at R=1.9 and 2.2m, respectively.

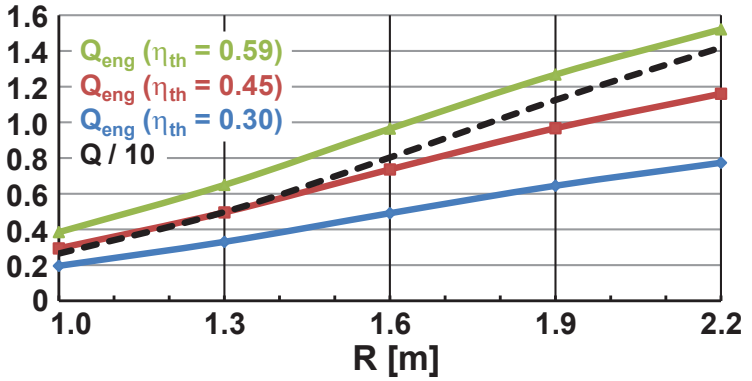

FIG. 3: Engineering and fusion gain versus device size for high-performance ST-FNSF scenarios.

Importantly, Figure 3 shows that as R is increased from 1m to 2.2m the smallest possible ST device that can achieve electricity break-even ($Q_{eng} \approx 1$) has R = 1.6m assuming very high blanket thermal conversion efficiency $\eta_{th} = 0.59$ as used in the ARIES-AT power plant design [12]. For $\eta_{th} = 0.45$, the required device size to achieve $Q_{eng} = 1$ increases to R=1.9-2m, and still larger devices are required for lower η_{th}. The auxiliary power for these higher performance scenarios is approximately 1/3 lower than for the cases shown in Figure 2, the fusion gain values are 3-4 times higher, and the fusion power levels are 2-3 times higher. From these studies it is concluded that an intermediate-scale ST-FNSF device with R=1.6m could hypothetically achieve Q_{eng} approaching 1 but would require very advanced physics and engineering performance.

3 Divertor Configuration

As described in Section 1, sufficient plasma shaping will be important for operating with sufficient stability margin for FNSF applications, and will be essential for accessing advanced operating modes with very high β and fusion performance as shown in Figure 3. In particular, achieving high triangularity δ is essential at high elongation to achieve high ST stability limits [13]. Further, increased triangularity generally increases peeling-ballooning limits and the achievable confinement in the H-mode pedestal region [14].

Achieving high-δ can be challenging in the ST configuration since at least one set of divertor poloidal field (PF) coils is required to be both inboard and close to the divertor x-point. This is challenging in a nuclear environment since neutron damage to the PF coil insulation can substantially reduce the lifetime of the insulator and hence the coil. Figure 4 shows a potential solution in which PF coils in a Bitter plate configuration are installed at the ends of the TF central rod and the CS shield and TF Cu conductor help shield the PF coils.

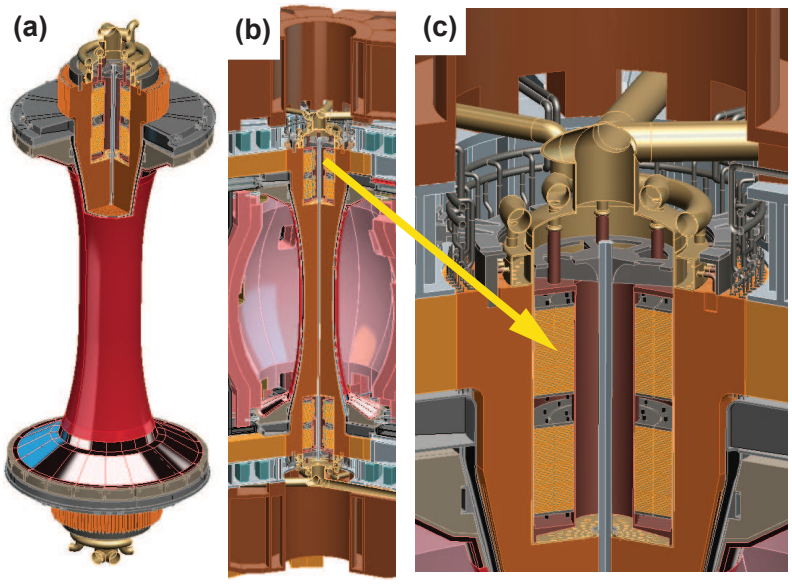

FIG. 4: (a) Centerstack removed from device, (b) centerstack installed in device, (c) divertor PF coils and manifolds in ends of TF.

Neutronics calculations for these PF coils find that for the R=1.6m FNSF scenario, the radiation level is 1.8×10^{10} Gy at 6 FPY for P_{fus} = 160MW. For the R=1.6m device with a pilot plant mission (P_{fus} = 420MW) the dose increases to 4.7×10^{10} Gy. Such doses are two orders of magnitude above allowable limits for organic insulators such as cynate ester. However, such doses are below the limits of some ceramic insulators such as MgO which has a limit above 10^{11} Gy [15]. Equilibrium calculations show that such PF coils at the ends of the TF can provide high triangularity = 0.55-0.6, and that this is sufficient to provide shaping factor S = 30 for q^*=3.8 FNSF scenarios and S = 20 for q^*=2.5 pilot plant scenarios.

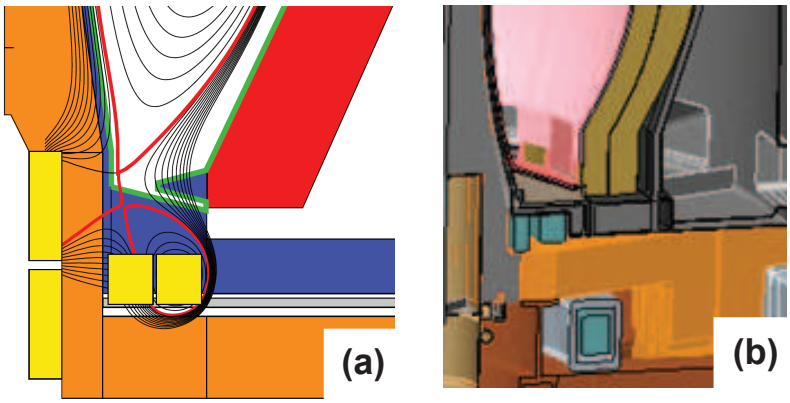

FIG. 5: (a) High-δ snowflake divertor plasma, (b) 3D rendering of lower divertor region including PF coils (teal) and blankets (pink).

Recent assessments of the divertor heat flux scaling in tokamaks [16, 17] finds an unfavorable scaling with plasma current in which the scrape-off-layer (SOL) heat flux width scales nearly inversely with plasma current. If realized, such SOL narrowing at high current projects to very narrow heat-flux channels and high peak heat flux values in next-step devices including ITER. A potential solution to the heat-flux challenge is increased flux expansion and field-line connection length in the divertor. Very high flux expansions of 40-60 in the "snowflake" divertor configuration have recently been shown to successfully reduce peak heat flux by a factor of 2-3 in NSTX, and the snowflake has also been observed to promote detachment which can further reduce the peak heat flux by an additional factor of 2 [18]. Figure 5a shows the PF coils (yellow), TF coils (orange), divertor shielding (blue), blanket modules (red), limiter outline (green), and poloidal flux contours (black) for a snowflake divertor in a R=1.6m ST-FNSF device. As is evident from the figure, a second x-point is present below the main x-point as is typical of the snowflake "minus" configuration. Figure 5b shows the 3D rendering of the divertor region with the snowflake divertor PF coils shown in green. The snowflake configuration shown in Figure 5a has a flux expansion of 60-70, and when combined with an assumed 70% core radiation fraction, upper-lower power splitting with a double-snowflake, and partial detachment, the peak heat flux is projected to be under engineering limits of 10MW/m^2.

4 Tritium Self-sufficiency

Achieving tritium self-sufficiency is an important requirement for a fusion system, and the relevant parameter for self-sufficiency is the tritium breeding ratio (TBR), i.e. the ratio of tritium bred to tritium consumed. A particular issue for smaller ST-FNSF devices is that it will likely be more difficult to achieve TBR = 1 since a higher fraction of in-vessel surface area must be dedicated to auxiliary heating ports and blanket test modules. To begin to analyze the dependence of TBR on device size, the TBR for a range of blanket configurations has been computed for the R=1.6m FNSF device. Figure 6 shows these blanket configurations and lists a TBR number for each. Figure 6a shows that the TBR of a straight blanket with a height comparable to the plasma height has TBR=0.8 which is significantly below 1 due to losses to the magnets and externals.

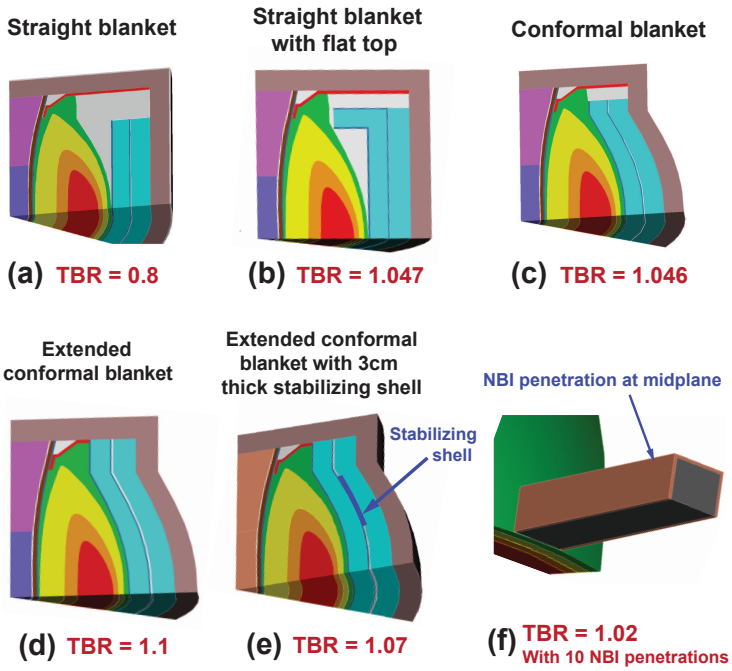

FIG. 6: Calculated TBR for various blankets for R=1.6m FNSF.

Additional calculations (not shown) for this blanket extended to the vacuum boundary increase the TBR to near 1, but this does not leave room at the top and bottom of the vessel for divertor pumping or maintenance or other manifolds. Figures 6b and c show that either the additional top/bottom blanket modules or having a conformal blanket can increase the TBR to 1.05. Figures 6d extends the conformal blanket to the top and bottom of the vessel. The 3D model of the R=1.6m design indicates that the slots in the ends of the blankets for divertor access and maintenance would modify the TBR to be approximately mid-way between the values in Figures 6c and d, i.e. the effective TBR = 1.073. Figure 6e shows that the inclusion of stabilizing shells for suppressing the vertical instability reduces TBR by approximately 0.03, and Figure 6f shows that 10 midplane NNBI penetrations of $0.36m^2$ each (assuming usage of the JT-60SA NNBI beam geometry) would further reduce the TBR by 0.05. Thus, the approximate TBR for the R=1.6m beam-driven ST-FNSF device is 1.073 - 0.03 - 0.05 = 0.993, i.e. very close to 1. Moving half of the NBI ports off midplane (as is planned) and optimizing the stabilizing shell for minimal TBR reduction should be sufficient to raise TBR > 1. This analysis indicates that R=1.6m is very close to the threshold for tritium self-sufficiency, and that smaller devices with relatively larger blanket penetrations may have difficulty achieving TBR = 1.

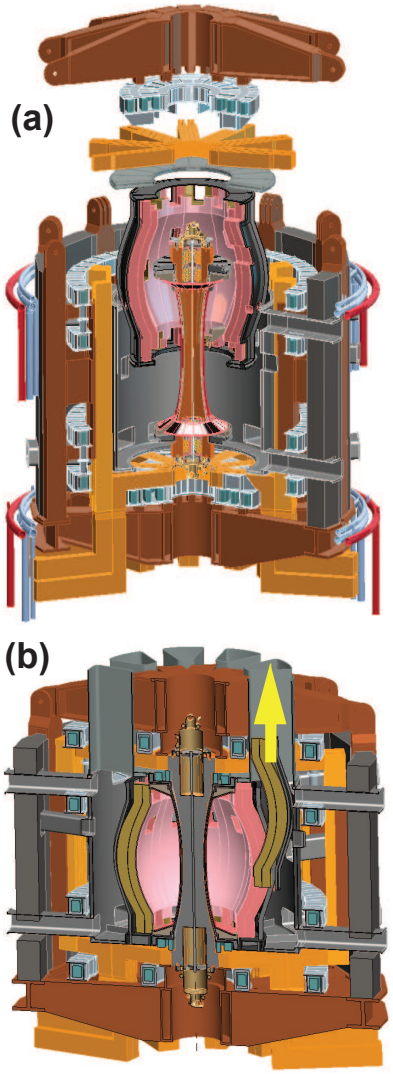

FIG. 7: Vertical maintenance concepts for R=1.6m FNSF.

5 Maintenance Strategies

A key potential advantage of the ST for FNSF applications is modularity of the overall configuration due in large part to the demountability of the normally conducting TF coils. The cylindrical geometry of the ST configuration naturally lends itself to a vertical maintenance strategy. For the PPPL ST Pilot/FNSF design, several design choices have been adopted to keep device design modular and similar to present-day devices such as MAST and NSTX wherever possible. Figure 7a shows the key components of the present proposed ST-FNSF design - namely individual outboard TF legs (orange) (in contrast to a continuous conducting shell and dome), a MAST-like cylindrical vacuum vessel (grey) with radial ports for NBI, test-blankets, and divertor access. Removable/re-weldable top and bottom discs complete the vacuum boundary. The vacuum vessel is chosen to be independent of the load-bearing structure (brown) that takes the electromagnetic forces from the coil fields and currents. Also shown is a blanket structure (pink) that can be lifted vertically as a single unit, a centerstack containing TF conductors and PF coils at the ends of the TF bundle, and superconducting poloidal field coils (teal) outboard of the centerstack.

Figure 7a shows that access to the blanket system requires removal of the top support, PF coils, TF horizontal legs, and vessel disc. For infrequent blanket maintenance or replacement of the entire blanket structure, such a maintenance approach is favorable. However, for more frequent blanket modifications (for example for replacement or repair during the testing phase of a new blanket module concept), a different access scheme may be preferable. Figure 7b shows a vertical maintenance scheme similar to that adopted for the AT pilot plant [3, 19] in which blanket sectors are translated radially, toroidally, and then vertically (see yellow upward pointing arrow) through permanent maintenance ports on top of the machine. The usage of such ports may provide faster and/or easier maintenance than removal of the entire top of the machine. In future designs it may be possible to combine both maintenance schemes enabling removal of either individual blanket sectors or the entire blanket structure. A final important result shown in Figure 7b is that the poloidal field coil positions consistent with this maintenance approach are compatible with the high-δ snowflake divertor equilibrium shown in Figure 5a.

6 Summary and Future Work

Preliminary studies of ST-FNSF performance dependence on device size find that a R=1.6m device can provide $\geq$ 1MW/m^2 neutron wall loading with global stability and confinement performance comparable to that already achieved on NSTX. This size device can also provide sufficient shielding for ceramic-insulated divertor coils needed for achieving high triangularity and a snowflake divertor. Analysis indicates that R=1.6m is the approximate minimum size that could access $Q_{eng} = 1$ and TBR = 1. Future studies will assess smaller R and develop more detailed physics scenarios and maintenance strategies.

References

[1] MENARD, J., et al., Nucl. Fus. **52** (2012) 083015.
[2] GERHARDT, S., ANDRE, R., and MENARD, J., Nucl. Fus. **52** (2012) 083020.
[3] MENARD, J. E., et al., Nucl. Fus. **51** (2011) 103014.
[4] PENG, Y.-K. M., et al., Plasma Phys. and Contr. Fus. **47** (2005) B263.
[5] PENG, Y.-K. M., et al., Fusion Sci. Technol. **56** (2009) 957.
[6] VOSS, G., et al., Fus. Engin. and Design **83** (2008) 1648.
[7] KOTSCHENREUTHER, M., et al., Fus. Engin. and Design **84** (2009) 83.
[8] KUTEEV, B., V., et al., Nucl. Fus. **51** (2011) 073013.
[9] GERHARDT, S., et al., paper EX/9-3, this conference.
[10] BERKERY, J. and et al., paper EX/P8-07, this conference.
[11] ABDOU, M., et al., Fus. Technol. **29** (1996) 1.
[12] NAJMABADI, F., et al., Fus. Engin. and Design **80** (2006) 3.
[13] MENARD, J. E., et al., Phys. Plasmas **11** (2004) 639.
[14] DIALLO, A. and et al., contributed oral NO4.00007, APS-DPP 2010.
[15] FAN, K., et al., R&D of a Septum Magnet Using MIC coil, Proceedings of the 5th Annual Meeting of Particle Accelerator Society of Japan and the 33rd Linear Accelerator Meeting in Japan (August 6-8, 2008, Higashihiroshima, Japan).
[16] EICH, T., et al., Phys. Rev. Lett. **107** (2011) 1.
[17] GOLDSTON, R., Nucl. Fus. **52** (2012) 013009.
[18] SOUKHANOVSKII, V., et al., paper EX/P5-21, this conference.
[19] BROWN, T., et al., PPPL report 4799 (2012).